

The magnetohydrodynamics model of twin kilohertz QPOs in LMXBs

Changsheng Shi^{1,2*} and Xiang-Dong Li¹

¹*Department of Astronomy, Nanjing University, Nanjing 210093, China;*

²*College of Material Science and Chemical Engineering, Hainan University, Hainan 570228, China*

Accepted ??; Received ??; in original form ??

ABSTRACT

We suggest an explanation for the twin kilohertz quasi-periodic oscillations (kHz QPOs) in low-mass X-ray binaries (LMXBs) based on magnetohydrodynamics (MHD) oscillation modes in neutron star magnetospheres. Including the effect of the neutron star spin, we derive several MHD wave modes by solving the dispersion equations, and propose that the coupling of the two resonant MHD modes may lead to the twin kHz QPOs. This model naturally relates the upper, lower kHz QPO frequencies with the spin frequencies of the neutron stars, and can well account for the measured data of six LMXBs.

Key words: accretion: accretion discs – X-rays: binaries – stars: magnetic fields

1 INTRODUCTION

The fastest variability components in X-ray binaries, the kilohertz quasi-periodic oscillations (kHz QPOs), have been detected in about thirty neutron star low-mass X-ray binaries (NS LMXBs) since first discovered with Rossi X-ray Timing Explorer in 1996 (see van der Klis 2006 for a review). Twin kHz QPOs appeared simultaneously in about twenty NS LMXBs. These QPOs are thought to reflect the motion of matter at the inner edge of an accretion disc around the NS. Early observations showed that the frequency separation ($\Delta\nu$) of the twin kHz QPOs is close to the NS spin frequency (ν_s) (e.g. Strohmayer et al. 1996; Ford et al. 1997), suggesting a beat-frequency explanation (Miller, Lamb & Psaltis 1998). However, the

* E-mail: scs1217@gmail.com

more detailed measurements revealed that $\Delta\nu$ is generally inconsistent with a constant value of ν_s but varying with the upper (ν_2) or lower (ν_1) frequency of the twin kHz QPOs (van der Klis et al. 1997; Méndez et al. 1998, 1999). Stella & Vietri (1999) propose a relativistic precession model which predicts a changing peak separation of the twin kHz QPOs. The upper and the lower kHz QPO frequencies are identified with the Keplerian frequency of the rotational plasma flow at the inner edge of the disc and the periastron precession frequency of the orbit, respectively. In this model, the NS spin frequency plays no role in setting up the frequencies of the kHz QPOs, but a massive ($\sim 2M_\odot$) NS is usually required to match the observations. Abramowicz et al. (2001, 2003) suggest that the twin kHz QPOs can be explained by a nonlinear resonance in the epicyclic motion in the accretion disc, leading to the 3 : 2 ratio of the upper and lower frequencies, although whether there is an intrinsically preferred ratio between the ν_2 and ν_1 is controversial (Belloni et al. 2007).

The subtle feature of twin kHz QPOs is that $\Delta\nu$ is variable but seems to be around either ν_s or $\nu_s/2$ (Smith, Morgan & Bradt 1997; Wijnands & van der Klis 1997; Markwardt, Strohmayer & Swank 1999; Chakrabarty et al 2003; Wijnands et al. 2003; Barret, Bouvier & Miller 2008; see, however, Yin et al. 2007; Méndez & Belloni 2007). This has motivated some scenarios of kHz QPOs taking into account the effect of the NS spin. Osherovich & Titarchuk (1999) suggest that kHz QPOs could be modeled as oscillations of the blobs thrown into magnetosphere from the inner edge of the accretion disc. The lower kHz QPO frequency ν_1 is identified as the Keplerian frequency in the disc and the upper frequency ν_2 the hybrid frequency about the Keplerian frequency and the NS spin frequency. Lee, Abramowicz & Kluźniak (2004) show that the kHz QPOs may be attributed to forcing of epicyclic motions in the accretion disc by the NS, which induces resonance at selected frequencies when the frequency separation $\Delta\nu$ is equal to ν_s or $\nu_s/2$. Li & Zhang (2005, see also Zhang 2004) present an alternative interpretation for the origin of the twin kHz QPOs by considering the interaction between the NS magnetic field and the surrounding accretion disc, which gives rise to MHD loop oscillations at the inner edge of the disc with the frequencies depending on the spin frequencies.

In this paper, we propose a model to explain kHz QPOs in NS LMXBs based on the interaction of accreting plasma with the NS magnetosphere. This model is partially based on the interpretation of Zhang (2004) and Reznia & Samson (2005). In the latter work it was argued that distortion of the NS magnetosphere by the infalling plasma of the Keplerian accretion flow can excite resonant shear Alfvén waves in a region of enhanced density gra-

dients, where accretion material flows along the magnetic field lines in the magnetosphere. The major difference between our model and Reznia & Samson's (2005) is that we have included the effect of the gravity and spin of the NS on the field line resonances.

This paper is organized as follows. In section 2 we introduce the basic physical model and derive the relation between ν_s , ν_1 and ν_2 . In section 3 we compare the theoretical relations with the observational data of six sources (4U 0614+09, 4U 1608–52, 4U 1636–53, 4U 1728–34, 4U 1915–05, and XTE 1807–294). In section 4 we summarized our results and discuss their possible implications.

2 THE MODEL

In LMXBs the plasma from the donor star accretes onto the NS via an accretion disc. Material in the disc firstly rotates in a Keplerian motion, then corotates with the magnetosphere after it is trapped completely by the NS magnetic field at the magnetospheric radius, and finally flows along the field lines to the polar cap. Some resonant modes may be excited by the perturbations at the magnetospheric radius when the plasma begins to corotate with the magnetosphere (Osherovich & Titarchuk 1999; Lee et al. 2004; Zhang 2004; Reznia & Samson 2005). We consider the QPOs as a modulation effect of the MHD waves which are produced at the magnetospheric radius, and the coupling of the two resonant MHD modes may lead to the twin kHz QPOs in the power spectrum.

We consider the MHD equations in a frame of reference corotating with the NS (shown in Fig. 1), written as follows (Landau & Lifshitz 1976)

$$\rho \frac{d\mathbf{v}}{dt} = -\nabla P + \mathbf{J} \times \mathbf{B} + 2\rho\mathbf{v} \times \boldsymbol{\Omega} + \rho\boldsymbol{\Omega} \times (\mathbf{r} \times \boldsymbol{\Omega}) - \rho \frac{GM}{r^3} \mathbf{r}, \quad (1)$$

$$\frac{\partial \mathbf{B}}{\partial t} = \nabla \times (\mathbf{v} \times \mathbf{B}) = (\mathbf{B} \cdot \nabla) \mathbf{v} - (\mathbf{v} \cdot \nabla) \mathbf{B} - (\nabla \cdot \mathbf{v}) \mathbf{B}, \quad (2)$$

$$\frac{\partial \rho}{\partial t} + \nabla \cdot (\rho \mathbf{v}) = 0, \quad (3)$$

$$P\rho^{-\gamma} = \text{const}, \quad (4)$$

where \mathbf{v} is the plasma velocity, \mathbf{J} electric current, \mathbf{B} magnetic field, \mathbf{r} the displacement from the center of the NS to the plasma, ρ plasma density, P barometric pressure, γ adiabatic index, G gravitational constant, M and $\boldsymbol{\Omega}$ the mass and the angular velocity of the NS¹,

¹ Actually $\boldsymbol{\Omega}$ is the angular velocity of the NS magnetosphere, which could be slightly deviate from that of the NS.

respectively. The third, fourth and fifth terms on the rhs of Eq. (1) represent the Coriolis force, the centrifugal force and the gravity, respectively.

Observationally the accretion rates in LMXBs change on a timescale of $\sim 10^3 - 10^4 s$. This is much more than the relaxation (or dynamic) timescale of the plasma at the inner disc radius ($\sim 10^{-2} - 10^{-3} s$). So we can approximate the plasma to be in an equilibrium state, which is subject to small perturbations, as discussed in Benz (2002). By use of the current expression,

$$\mathbf{J} = \frac{1}{\mu} \nabla \times \mathbf{B}, \quad (5)$$

where μ is vacuum magnetic conductivity, Eqs. (1)-(3) can be transformed to be

$$\rho_0 \frac{\partial \mathbf{v}_0}{\partial t} + (\mathbf{v}_0 \cdot \nabla) \mathbf{v}_0 = -\nabla P_0 + \frac{1}{\mu} (\nabla \times \mathbf{B}_0) \times \mathbf{B}_0 + 2\rho_0 \mathbf{v}_0 \times \boldsymbol{\Omega} + \rho_0 \Omega^2 \mathbf{r}_0 - \rho_0 (\boldsymbol{\Omega} \cdot \mathbf{r}_0) \boldsymbol{\Omega} - \rho_0 \frac{GM}{r_0^3} \mathbf{r}_0, \quad (6)$$

$$\frac{\partial \mathbf{B}_0}{\partial t} = (\mathbf{B}_0 \cdot \nabla) \mathbf{v}_0 - (\mathbf{v}_0 \cdot \nabla) \mathbf{B}_0 - (\nabla \cdot \mathbf{v}_0) \mathbf{B}_0, \quad (7)$$

$$\frac{\partial \rho_0}{\partial t} + \nabla \cdot (\rho \mathbf{v}_0) = 0, \quad (8)$$

where the subscript 0 denotes variables in the equilibrium state. The initial relative velocity (\mathbf{v}_0) is equal to zero in the corotating reference system and can be expressed as $\boldsymbol{\Omega} \times \mathbf{r}_0$ in the inertial reference system.

Now we consider the MHD equations for the plasma subject to small perturbations,

$$\rho_0 \frac{\partial \hat{\mathbf{v}}}{\partial t} + (\hat{\mathbf{v}} \cdot \nabla) \hat{\mathbf{v}} = -\nabla \hat{P} + \frac{1}{\mu} (\nabla \times \hat{\mathbf{B}}) \times \hat{\mathbf{B}} + 2\rho_0 \hat{\mathbf{v}} \times \boldsymbol{\Omega} + \rho_0 \Omega^2 \hat{\mathbf{r}} - \rho_0 (\boldsymbol{\Omega} \cdot \hat{\mathbf{r}}) \boldsymbol{\Omega} - \rho_0 \frac{GM}{r_0^3} \hat{\mathbf{r}}, \quad (9)$$

$$\frac{\partial \hat{\mathbf{B}}}{\partial t} = (\hat{\mathbf{B}} \cdot \nabla) \hat{\mathbf{v}} - (\hat{\mathbf{v}} \cdot \nabla) \hat{\mathbf{B}} - (\nabla \cdot \hat{\mathbf{v}}) \hat{\mathbf{B}}. \quad (10)$$

$$\frac{\partial \hat{\rho}}{\partial t} + \nabla \cdot (\hat{\rho} \hat{\mathbf{v}}) = 0, \quad (11)$$

$$\hat{P} \hat{\rho}^{-\gamma} = P_0 \rho_0^{-\gamma}, \quad (12)$$

where $\hat{\mathbf{v}} = \mathbf{v}_0 + \mathbf{v}_s = \mathbf{v}_s$, $\hat{\mathbf{B}} = \mathbf{B}_0 + \mathbf{B}_s$, $\hat{\mathbf{r}} = \mathbf{r}_0 + \mathbf{r}_s$, $\hat{\rho} = \rho_0 + \rho_s$, $\hat{P} = P_0 + P_s$ with the subscript s denoting the perturbed quantities ($v_s \ll |\boldsymbol{\Omega} \times \mathbf{r}_0|$, $B_s \ll B_0$, $r_s \ll r_0$, $\rho_s \ll \rho_0$, $P_s \ll P_0$) and with the superscript ^ the variables after the disturbance. Combining Eqs. (6)-(12) we get the equations about the perturbed quantities in the first order approximation,

$$\begin{aligned} \rho_0 \frac{\partial \mathbf{v}_s}{\partial t} &= -\frac{\gamma P_0}{\rho_0} \nabla \rho_s + \frac{1}{\mu} [(\nabla \times \mathbf{B}_0) \times \mathbf{B}_s + (\nabla \times \mathbf{B}_s) \times \mathbf{B}_0] + 2\rho_0 \mathbf{v}_s \times \boldsymbol{\Omega} + \rho_0 \Omega^2 \mathbf{r}_s \\ &\quad - \rho_0 (\boldsymbol{\Omega} \cdot \mathbf{r}_s) \boldsymbol{\Omega} - \rho_0 \frac{GM}{r_0^3} \mathbf{r}_s, \end{aligned} \quad (13)$$

$$\frac{\partial \mathbf{B}_s}{\partial t} = (\mathbf{B}_0 \cdot \nabla) \mathbf{v}_s - (\nabla \cdot \mathbf{v}_s) \mathbf{B}_0, \quad (14)$$

and

$$\frac{\partial \rho_s}{\partial t} + \rho_0 \nabla \cdot \mathbf{v}_s = 0. \quad (15)$$

Differentiating Eq. (13) and substituting $\nabla(\mathbf{B}_0 \cdot \mathbf{B}_s) = (\mathbf{B}_0 \cdot \nabla)\mathbf{B}_s + (\mathbf{B}_s \cdot \nabla)\mathbf{B}_0 + \mathbf{B}_s \times (\nabla \times \mathbf{B}_0) + \mathbf{B}_0 \times (\nabla \times \mathbf{B}_s)$ into it give

$$\begin{aligned} \rho_0 \frac{\partial^2 \mathbf{v}_s}{\partial t^2} = & -\frac{\gamma P_0}{\rho_0} \frac{\partial}{\partial t} (\nabla \rho_s) + \frac{1}{\mu} \frac{\partial}{\partial t} [(\mathbf{B}_0 \cdot \nabla)\mathbf{B}_s + (\mathbf{B}_s \cdot \nabla)\mathbf{B}_0 - \nabla(\mathbf{B}_0 \cdot \mathbf{B}_s)] \\ & + 2\rho_0 \frac{\partial}{\partial t} (\mathbf{v}_s \times \boldsymbol{\Omega}) + \rho_0 \Omega^2 \mathbf{v}_s - \rho_0 (\boldsymbol{\Omega} \cdot \mathbf{v}_s) \boldsymbol{\Omega} - \rho_0 \frac{GM}{r_0^3} \mathbf{v}_s. \end{aligned} \quad (16)$$

We assume that (1) the accretion disc is infinitesimally thin, (2) the magnetic moment and the spin of the NS are parallel to the z axis, and normal to the disc, i.e., $\mathbf{B}_0 = (0, 0, B_0)$ and $\boldsymbol{\Omega} = (0, 0, \Omega)$ close to the inner edge of the disc, and (3) the x and y axes are along the disc plane, and the MHD wave is assumed to propagate in the xoz plane, i.e., the wave vector $\mathbf{k} = (k \sin \theta, 0, k \cos \theta)$, where θ is the angle between the z axis and \mathbf{k} . After carrying out Fourier transformation for Eqs. (14)-(16) we get the following dispersion equations,

$$\left(1 + \frac{\Omega^2}{\omega^2} - \frac{\omega_k^2}{\omega^2} - \frac{k^2 V_A^2}{\omega^2} - \frac{k^2 c_s^2 \sin^2 \theta}{\omega^2}\right) v_{sx} = \frac{k^2 c_s^2 \sin \theta \cos \theta}{\omega^2} v_{sz} + \frac{2\Omega i}{\omega} v_{sy}, \quad (17)$$

$$\left(1 + \frac{\Omega^2}{\omega^2} - \frac{\omega_k^2}{\omega^2} - \frac{k^2 V_A^2 \cos^2 \theta}{\omega^2}\right) v_{sy} = -\frac{2\Omega i}{\omega} v_{sx}, \quad (18)$$

$$\left(1 - \frac{\omega_k^2}{\omega^2} - \frac{k^2 c_s^2 \cos^2 \theta}{\omega^2}\right) v_{sz} = \frac{k^2 c_s^2 \sin \theta \cos \theta}{\omega^2} v_{sx}, \quad (19)$$

where i is imaginary unit, $V_A (= \sqrt{B_0^2 / \mu \rho_0})$, $c_s (= \sqrt{\gamma P_0 / \rho_0})$, $\omega_k (= \sqrt{GM / r_0^3})$, and ω are Alfvén velocity, acoustic velocity, Keplerian angular velocity, and angular velocity of the perturbation at r_0 respectively, and v_{sx} , v_{sy} , v_{sz} are the three components of the perturbed quantity of the speed. Equations (17)-(19) show that there exist three resonance MHD modes. At the magnetospheric radius r_0 , the magnetic energy density is equal to the total kinetic energy density, i.e. $B^2 / 8\pi = \rho V_A^2 / 2 \simeq \rho V_K^2 / 2$ (Davidson & Ostriker 1973; Ghosh et al. 1977). Since the characteristic wavelength is in the same order with the magnetospheric radius (Rezania & Samson 2005), we then have $kV_A \sim kV_K \sim V_K / r_0 = \omega_k$, or $kV_A = \eta \omega_k$. Because the thermal pressure of the plasma might be comparable with the magnetic pressure ($c_s \sim V_A$) just inside the magnetosphere (Miller et al. 1998), we also suppose $kc_s = \lambda \omega_k$. Here both η and λ are taken to be constant for certain sources. Substitute these relations into Eqs. (17)-(19) we can get the resonant modes. Specifically when $\theta = 0$, from Eqs. (17) and (18) we can get $v_{sx} = \pm i v_{sy}$, i.e. $v_{sx} e^{i\mathbf{k} \cdot \mathbf{r} - i\omega t} = v_{sy} e^{i\mathbf{k} \cdot \mathbf{r} - i\omega t \pm i\frac{\pi}{2}}$. Substituting this relation into the Eqs. (17)-(19) can give

$$\omega_1 = \sqrt{1 + \eta^2} \omega_k - \Omega, \quad (20)$$

$$\omega_2 = \sqrt{1 + \lambda^2} \omega_k, \quad (21)$$

$$\omega_3 = \sqrt{1 + \eta^2} \omega_k + \Omega, \quad (22)$$

where the negative solutions are excluded. Similarly when $\theta = \pi/2$,

$$\omega_1^2 = \omega_k^2, \quad (23)$$

$$\omega_2^2 = \omega_k^2 + \Omega^2 + \frac{\omega_k^2}{2}(\eta^2 + \lambda^2) + \frac{\omega_k}{2} \sqrt{\omega_k^2(\eta^2 + \lambda^2)^2 + 8\Omega^2(\eta^2 + \lambda^2 + 2)}, \quad (24)$$

$$\omega_3^2 = \omega_k^2 + \Omega^2 + \frac{\omega_k^2}{2}(\eta^2 + \lambda^2) - \frac{\omega_k}{2} \sqrt{\omega_k^2(\eta^2 + \lambda^2)^2 + 8\Omega^2(\eta^2 + \lambda^2 + 2)}. \quad (25)$$

Note that in the latter case the MHD wave couldn't propagate very far in the accretion disc, so we consider the coupling modes that propagate along the z axis ($\theta = 0$) as a more promising explanation of the QPOs.

We first rule out the possibility of the ω_2 mode as the lower kHz QPOs, since Eq. (21) requires that it should always higher than Ω for stable accretion, which is contradicted with observations. The coupling between ω_1 and ω_3 can also be excluded, which implies a constant frequency separation. So we suggest the upper and the lower kHz QPO frequencies be $\nu_2 = \omega_2/2\pi$ and $\nu_1 = \omega_1/2\pi$. From Eqs. (20) and (21) we can get the following relation between the frequencies of the upper and the lower kHz QPOs,

$$\nu_2 = \sqrt{\frac{1 + \lambda^2}{1 + \eta^2}}(\nu_1 + \nu_s) \quad (26)$$

where $\nu_s = \Omega/2\pi$, or

$$\frac{\nu_2}{\nu_s} = \frac{1}{\sqrt{1 + \varepsilon^2}} \left(\frac{\nu_1}{\nu_s} + 1 \right) \quad (\text{when } \eta > \lambda), \quad (27)$$

$$\frac{\nu_2}{\nu_s} = \sqrt{1 + \delta^2} \left(\frac{\nu_1}{\nu_s} + 1 \right) \quad (\text{when } \eta < \lambda), \quad (28)$$

where $\varepsilon^2 = (\eta^2 - \lambda^2)/(1 + \lambda^2)$ and $\delta^2 = (\lambda^2 - \eta^2)/(1 + \eta^2)$. Equations (27) and (28) indicate that the twin kHz QPOs may be divided into two groups, with the slope of the ν_2/ν_s vs. ν_1/ν_s relation either larger or smaller than 1. In the following we call them the large slope coefficient sources (LSCS) and the small slope coefficient sources (SSCS), respectively.

3 COMPARISON WITH OBSERVATIONS

We compare in Fig. 2 the ν_2/ν_s vs. ν_1/ν_s relations obtained in last section with the observed kHz QPOs in six sources 4U 0614+09, 4U 1608–52, 4U 1636–53, 4U 1728–34, 4U 1915–05, XTE 1807–294, in which both the spin and twin kHz QPO frequencies have been measured. The spin frequencies, disposed in Table 1, are from van der Klis (2006), Méndez & Belloni (2007), Yin et al. (2007), Altamirano et al. (2008), and their references. For 4U 0614+09 we

adopt the updated spin frequency of 415 Hz (Strohmayer, Markwardt & Kuulkers 2008). The dots with error bars represent the measured values, and the solid lines stand for theoretical relations. We distinguish the ν_2/ν_s vs. ν_1/ν_s relations for SSCS and LSCS, and accordingly adopt relation (27) to fit the data for 4U 0614+09, 4U 1608–52, 4U 1636–53, and 4U 1728–34, and relation (28) for the other two sources, 4U 1915–05 and XTE 1807–294. For each source, the value of ε or δ for best fitting is also shown in the figure. It is noted that a cluster of the values ($\sim 0.3-0.9$) of ε and δ can well reproduce the observed relations. In the left panel of Fig. 3 we show the observed and predicted relations for all of the six sources. In the right panel we plot the relation between $\Delta\nu/\nu_s$ and ν_1/ν_s by use of the parameter ε or δ that we have got.

For SSCS the peak separation of the twin kHz QPOs is less than the spin frequency, i.e., $\Delta\nu - \nu_s = -(1 - 1/\sqrt{1 + \varepsilon^2})(\nu_1 + \nu_s) < 0$, and decreases with ν_1 or ν_2 ; for LSCS the peak separation is more than the spin frequency, i.e., $\Delta\nu = (\sqrt{1 + \delta^2} - 1)\nu_1 + \nu_s > \nu_s$, and increases with the increasing ν_1 or ν_2 . In the former group, $\Delta\nu$ is around ν_s for 4U 0614+09 and 4U 1728–34, and $\nu_s/2$ for 4U 1608–52 and 4U 1636–53 (Miller et al. 1998; van der Klis 1997; Stella, Vietri & Morsink 1999; Lewin & van der Klis 2006; M’endez & Belloni 2007).

Our final note is that when the Alfvén speed is equal to the acoustic speed of the plasma, i.e. $\eta = \lambda$, Eq. (26) will recover to the expression in the sonic-point beat-frequency model (Miller et al. 1998). In this case the peak separation is equal to the spin frequency and almost invariant.

4 DISCUSSION AND CONCLUSIONS

In this paper we propose a resonant MHD model for the twin kilohertz QPOs in LMXBs. The modes of the MHD waves vertical and parallel to the accretion disc are derived, and the twin kHz QPOs frequencies are identified with the frequencies of the two resonant modes. In this model the twin kHz QPO frequencies are correlated with the spin frequencies, and the separation frequencies also change with the QPO frequencies. We show that the measured relations between ν_1 , ν_2 , and ν_s can be accounted for with reasonable values of the input parameters.

There are several spin-involved MHD models for kHz QPOs in the literature. Osherovich & Titarchuk (1999) suggest that kHz QPOs can be explained as oscillations of large scale inhomogeneities (hot blobs) thrown into the NS magnetosphere. Participating in the radial

oscillations with Keplerian frequency, such blobs are simultaneously under the influence of the Coriolis force. The derived frequency relation is $\nu_2^2 = \nu_1^2 + (2\nu_s)^2$, or $(\nu_2/\nu_s)^2 = (\nu_1/\nu_s)^2 + 4$, which is plotted in the dotted curve in Fig. 4. The significant deviation from the measured data indicates that this model is not successful for most of the LMXBs. In their MHD loop oscillation model Li & Zhang (2005) derive a linear frequency relation, i.e., $\nu_2/\nu_s = \xi\nu_1/\nu_s + 1$ where $\xi \sim 1$ is an input parameter. Here the upper kHz QPO frequency is assumed to the Keplerian frequency and the lower kHz QPO is identified as the principal fast kink mode of the standing MHD waves along the toroidal field lines at the magnetospheric radius. The relation is also plotted in Fig. 4 in solid curves. A comparison with the measured data shows that the fit is acceptable for all the six sources.

Rezania & Samson (2005) propose a model for QPOs in LMXBs based on oscillating magnetohydrodynamic modes in NS magnetospheres. They argue that the interaction of the accretion disc with the magnetosphere can excite resonant shear Alfvén waves in a region of enhanced density gradients, where accretion material flows along the magnetic field lines in the magnetosphere. The predicted ν_2/ν_1 ratio is found to be independent of the NS spin frequencies. The main difference between Rezania & Samson (2005) and this work lies in that Rezania & Samson (2005) assume that the strong gravity of the NS produces a converging flow which will hit the star’s magnetosphere in a large velocity, while we consider the motion of the plasma is still mainly Keplerian, before they enter the magnetosphere and corotate with the magnetosphere. We also include the effect of the gravity and the rotation of the NS for the trapped plasma, and find that the resulting wave frequencies relate with both the spin frequency and the gravity.

So far we have assumed that the spin and magnetic axes of the NS are aligned in LMXBs. However, the existence of persistent millisecond pulsations in some LMXBs indicates that the magnetic axis is at least somewhat tilted from the spin axis. In this case the magnetic field is no longer homogeneous at a given radius in the accretion disc, and the orbit of plasma in the inner region of the disc becomes non circular. Furthermore, the stellar magnetic field can induce disk warping and precession (e.g. Lai 1999, 2003), and modulate the orbit and hence the QPO frequencies. For X-ray binaries the disc precession timescale is usually of tens of days to years (cf. Wijers & Pringle 1999 and references therein), which is much longer than the duration of each QPO observation. Additionally for accretion-powered millisecond pulsars the magnetic inclination is likely to be very small (Lamb et al., 2008). For the above

reasons we expect that the change of the QPO frequencies induced by oblique magnetic fields might be very small compared with the uncertainties in the measured frequencies.

Our results indicate that the peak separation is always related to the spin frequency. What's more, there seems to be a weak positive correlation between the spin frequency and the parameter ε for SSCS, which can be described as $\varepsilon = 2.28(\pm 0.16)(\nu_s/1000 \text{ Hz}) - 0.53(\pm 0.08)$, plotted in the left panel of Fig. 5. Substitute this relation into $\Delta\nu = (1/\sqrt{1+\varepsilon^2})(\nu_1 + \nu_s) - \nu_1$ we get a trend of $\Delta\nu$ changing with the spin frequency, as plotted in the right panel of Fig. 5. From the dark black curve to the light gray curve ν_1 changes from 1000 Hz to 100 Hz in a step of 100 Hz. We find that when ν_s increases, $\Delta\nu$ varies from $\sim \nu_s/2$ to $\sim \nu_s$, and finally to $\sim \nu_s/2$. The transitions occur at $\nu_s \sim 100$ Hz and 500 Hz, respectively.

The accretion process can take place only when the magnetospheric radius is less than the corotation radius (e.g. Ghosh & Lamb 1979). In other words, the Keplerian frequency at the magnetosphere radius should be more than the spin frequency of the NS if accretion process can take place. Because of this there is a minimum value of the lower frequency of the twin kHz QPOs in SSCS, $\nu_1 > (\sqrt{1+\varepsilon^2} - 1)\nu_s$. Besides, due to the fact that the peak separation must be positive values we can get the maximal value for the upper frequency, $\nu_2 < \nu_s/(\sqrt{1+\varepsilon^2} - 1)$ for SSCS. These may serve as possible evidence to testify this model with future measurements of kHz QPOs in LMXBs.

ACKNOWLEDGEMENTS

The authors thank the anonymous referee for the helpful suggestion on the manuscript. This work was supported by the Natural Science Foundation of China under grant numbers 10573010 and 10221001.

REFERENCES

- Abramowicz M.A., Kluzniak W., 2001, *A&A*, 374, L19
 Abramowicz M.A., Bulik T., Bursa M., Kluzniak W., 2003, *A&A*, 404, L21
 Altamirano D., van der Klis M., Méndez M., Jonker P.G., Klein-Wolt M., Lewin W. H. G., 2008, *ApJ*, accepted (astro-ph/0806.0962)
 Barret D., Boutelier M., Miller M.C., 2008, *MNRAS*, 384, 1519B
 Belloni T., Homan J., Motta S., Ratti E., Méndez M., 2007, *MNRAS*, 379, 247B
 Benz A.O., 2002, *Plasma Astrophysics: Kinetic Processes in Solar and Stellar Coronae*, 2nd

- edition, Astrophysics and Space Science Library, Vol. 279, Kluwer Academic Publishers, Dordrecht
- Boirin L., Barret D., Olive J.F., Bloser P.F., Grindlay J.E., 2000, *A&A*, 361, 121
- Boutloukos S., Lamb F.K., 2008, *AIPC*, 983, 533
- Boutloukos S., van der Klis M., Altamirano D., Klein-Wolt M., Wijnands R., Jonker P.G., Fender R.P., 2006, *ApJ*, 653, 1435B
- Chakrabarty D., Morgan E.H., Munro, M.P., Galloway D.K., Wijnands R., van der Klis M., Markwardt C.B. 2003, *Nature*, 424, 42
- Davidson K., Ostriker J.P. 1973, *ApJ*, 179, 585
- Di Salvo, T., Méndez M., van der Klis M., Ford E., Robba N.R., 2001, *ApJ*, 546, 1107
- Di Salvo T., Méndez M., van der Klis M., 2003, *A&A*, 406, 177
- Ford E.C. et al., 1997, *ApJ*, 486, 47
- Galloway D.K., Chakrabarty D., Munro M.P., Michael P., Savov P., 2001, *ApJ*, 549, 85
- Ghosh P., Lamb F.K., 1979, *ApJ*, 232, 259
- Ghosh P., Lamb F.K., Pethick C.J., 1977, *ApJ*, 217, 578
- Jonker P.G., Méndez M., van der Klis M., 2000, *ApJ*, 540, 29
- Jonker P.G., Méndez M., van der Klis M., 2002, *MNRAS*, 336, L1
- Lai D., 1999, *ApJ*, 524, 1030
- Lai D., 2003, *ApJ*, 591, L119
- Lamb F.K., Miller M.C. 2001, *ApJ*, 554, 1210
- Lamb F.K., Boutloukos S., Van W.S., Chamberlain R.T., Lo K.H., Clare A., Yu W.F., Miller M.C., 2008, submitted to *ApJ* (astro-ph/0808.4159)
- Landau L.D., Lifshitz E.M., 1976, *Mechanics*, 3rd edition, Course of Theoretical Physics, Vol. 1, Pergamon Press, Oxford and New York
- Lee W.H., Abramowicz M.A., Kluźniak W., 2004, *ApJ*, 603, L93
- Lee U., 2008, *MNRAS*, 385, 2069
- Li X.D., Zhang C.M., 2005, *ApJ*, 635, L57
- Linares M., van der Klis M., Altamirano D., Markwardt C.B. 2005, *ApJ*, 634, 1250
- Markwardt C.B., Strohmayer T.E., Swank J. H., 1999, *ApJ*, 512, L125
- Méndez M., Belloni T. 2007, *MNRAS*, 381, 790
- Méndez M., van der Klis M., 1999, *ApJ*, 517, L51
- Méndez M., van der Klis M., Wijnands R., Ford E.C., van Paradijjs J., Vaughan B.A., 1998, *ApJ*, 505, L23

- Migliari S., van der Klis M., Fender R.P., 2003, MNRAS, 345, L35
- Miller M.C., Lamb F.K., Psaltis D., 1998, ApJ, 508, 791
- Osherovich V., Titarchuk L., 1999, ApJ, 522, L113
- Psaltis D. et al., 1998, ApJ, 501, L95
- Rezania V., Samson J.C., 2005, A&A, 436, 999
- Smith D.A., Morgan E.H., Bradt H., 1997, ApJ, 479, L137
- Stella L., Vietri M., 1999, Phys. Rev. Lett., 82, 17
- Stella L., Vietri M., Morsink S., 1999, ApJ, 524, L63
- Strohmayer T.E., Zhang W., Swank J.H., Smale A., Titarchuk L., Day, C., Lee U., 1996, ApJ, 469, L9
- Strohmayer T.E., Markwardt C.B., Kuulkers E., 2008, ApJ, 672, L37-L40
- van der Klis M., Wijnands R.A.D., Horne K., Chen W., 1997, ApJ, 481, L97
- van der Klis M., 2006, in Lewin W. H. G., van der Klis M., eds, Compact Stellar X-ray Sources. Cambridge Univ. Press, Cambridge, p. 39
- van Straaten S., Ford E.C., van der Klis M., Méndez M., Kaaret P., 2000, ApJ, 540, 1049
- van Straaten S., van der Klis M., di Salvo T., Belloni T., Psaltis D., 2002, ApJ, 568, 912
- van Straaten S., van der Klis M., Méndez M., 2003, ApJ, 596, 1155
- Wijers R. A. M. J., Pringle J. E. 1999, MNRAS, 308, 207
- Wijnands R.A.D., van der Klis M., 1997, ApJ, 482, L65
- Wijnands R.A.D., van der Klis M., van paradijs J., Lewin W.H.G., Lamb F.K., Vaughan B., Kuulkers E., 1997, ApJ, 479, L141
- Wijnands R.A.D., van der Klis M., Homan J., Chakrabarty D., Markwardt C.B., Morgan E.H., 2003, Nature, 424, 44
- Yin H.X., Zhang C.M., Zhao Y.H., Lei Y.J., Qu J.L., Song L.M., Zhang F., 2007, A&A, 471, 381
- Zhang C.M., 2004, A&A, 423, 401
- Zhang F., Qu J., Zhang C.M., Chen W., Li T.P., 2006, ApJ, 646, 1116

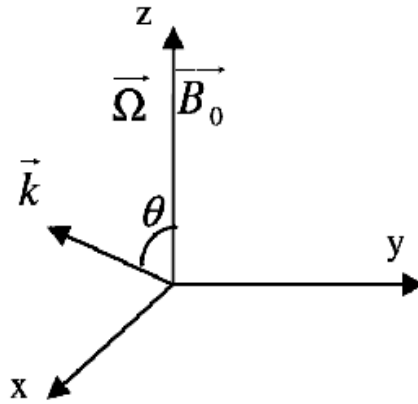


Figure 1. The coordinate system centered at the magnetospheric radius. The x axis is along the radial direction, y axis the toroidal direction, and the z axis is normal to the accretion disc.

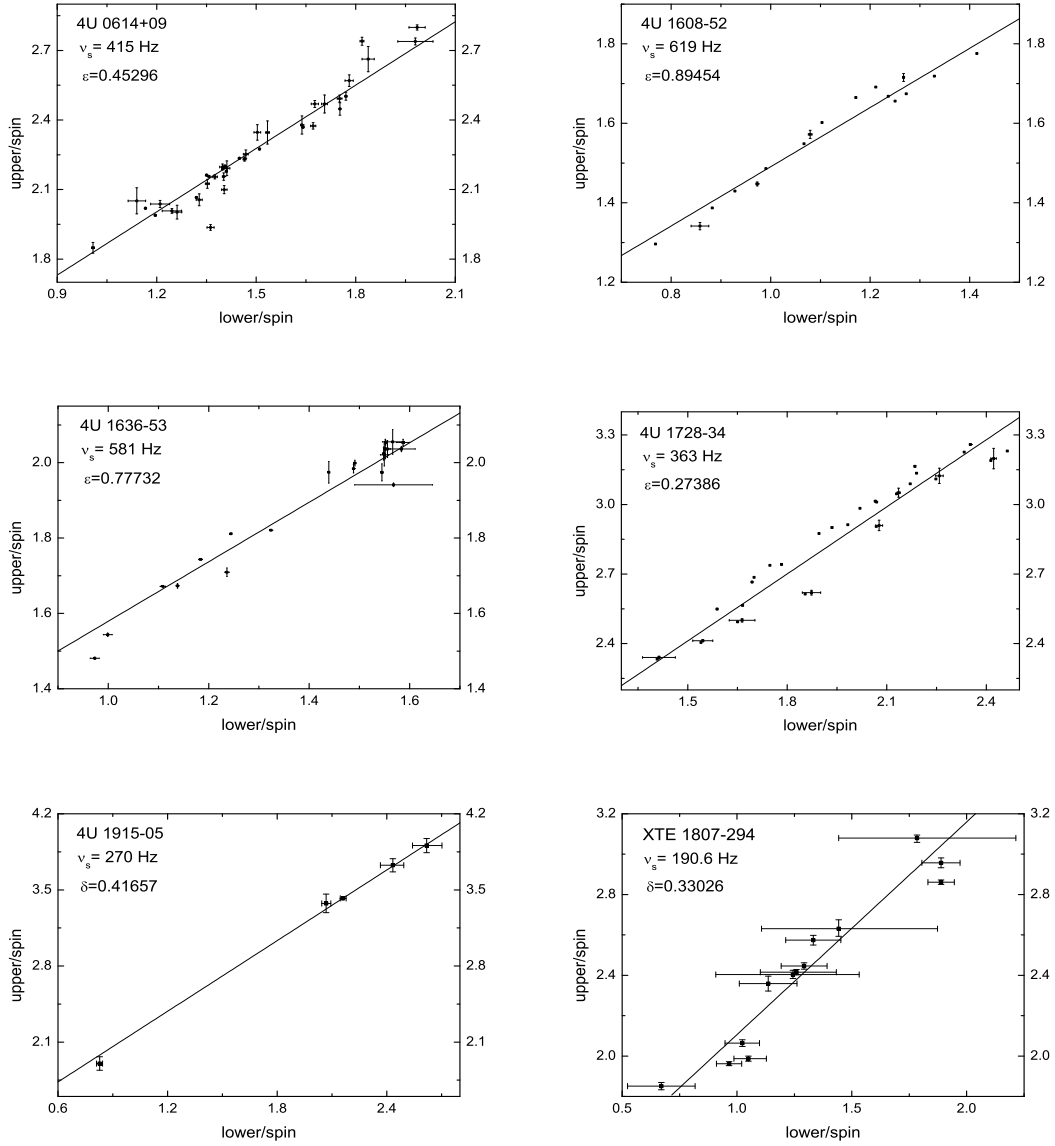


Figure 2. The relations between ν_2/ν_s and ν_1/ν_s for the six sources (for the measured data of 4U 0614+09: van Straaten et al. 2000; van Straaten et al. 2002; 4U 1608-52: van Straaten, van der Klis & Méndez 2003; 4U 1636-53: Altamirano et al., 2008; Di Salvo, Méndez et & van der Klis 2003; Jonker, Méndez & van der Klis 2002; Wijands et al. 1997; 4U 1728-34: Migliari, van der Klis & Fender 2003; Di Salvo et al. 2001; Jonker, Méndez & van der Klis 2000; 4U 1915-05: Boirin et al. 2000; XTE 1807-294: Linares et al. 2005; Zhang et al. 2006).

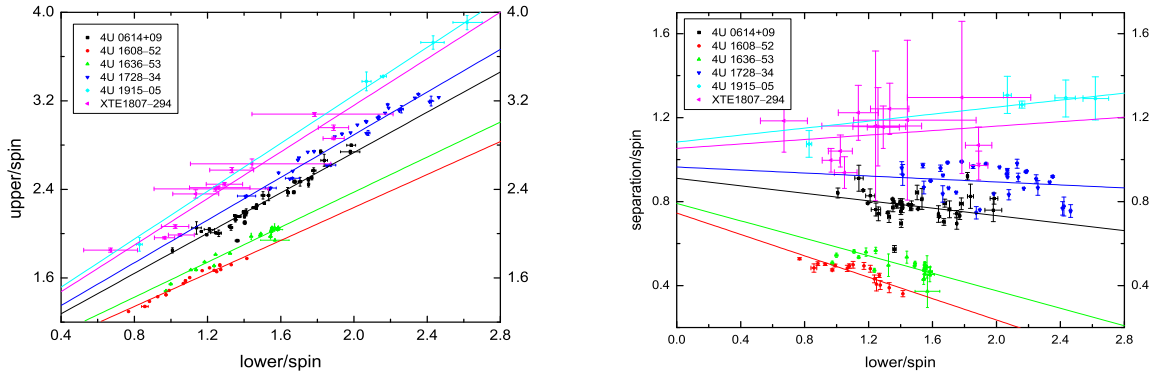


Figure 3. *Left* The relation between ν_2/ν_s and ν_1/ν_s . *Right* The relation between $\Delta\nu/\nu_s$ and ν_1/ν_s .

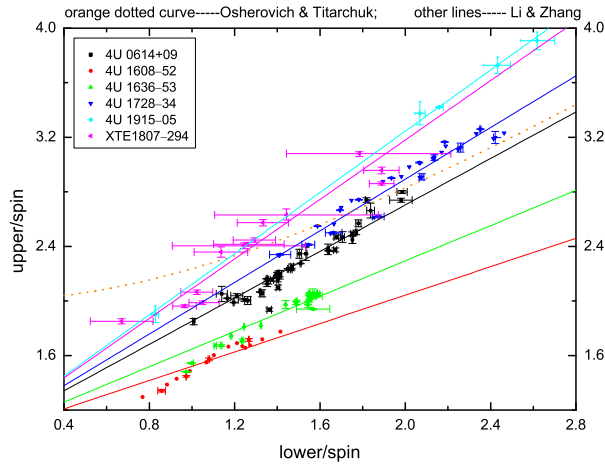


Figure 4. The relations between ν_2/ν_s and ν_1/ν_s compared with the predicted ones in Li & Zhang (2005) and Osherovich & Titarchuk (1999).

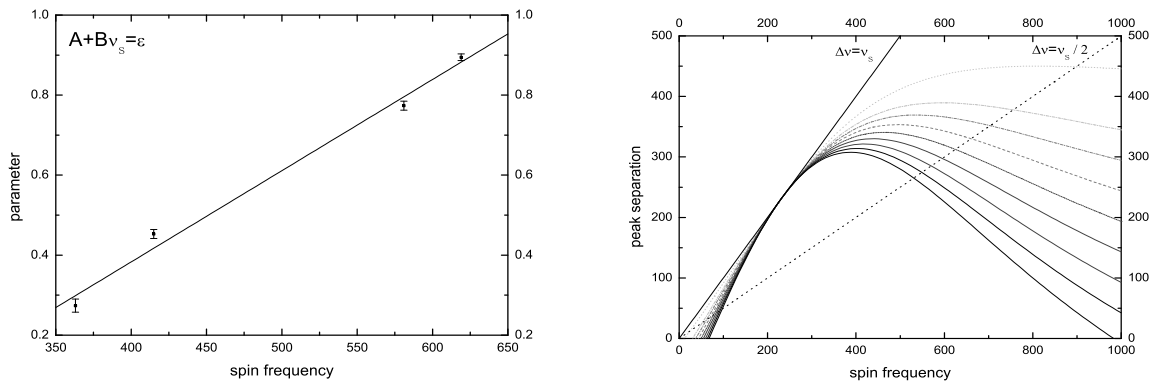


Figure 5. *Left* The relation between the parameter ε and the NS spin frequencies in the four SSCS. *Right* The relation between the peak separation of the twin kHz QPOs and the spin frequencies with different lower kHz QPO frequencies.

Table 1. The measured and fitted parameters for six LMXBs. For the first four sources we use the relation $\nu_2 = (\nu_1 + \nu_s)/(\sqrt{1 + \varepsilon^2})$, and for the last two sources with $\nu_2 = \sqrt{1 + \delta^2}(\nu_1 + \nu_s)$.

sources	ν_s (Hz)	ε or δ	error(\pm)	χ^2/DoF	slope
4U 1728–34	363	0.27386	0.01629	550.3/33	0.96449
4U 1608–52	619	0.89454	0.00826	450.5/16	0.74531
4U 1636–53	581	0.77732	0.00768	551.3/24	0.78953
4U 0614+09	415	0.45296	0.01118	563.0/39	0.91091
4U 1915–05	270	0.41657	0.01784	840.3/ 4	1.08330
XTE 1807–294	190.6	0.33026	0.04213	94.6/12	1.05312